Optical Characterization of Calcium Fluoride and Grey Tin using Spectroscopic Ellipsometry

Jaden R. Love

BE BOLD. Shape the Future.®
New Mexico State University

Acknowledgments

Committee Members:

- Stefan Zollner, PhD (Chair)
- Michael Engelhardt, PhD
- Ludi Miao, PhD
- Corey Frank, PhD

Current Research Team:

- Carlos Armenta, PhD
- Haley Woolf, B.S.
- Yoshitha Hettige, M.S.
- Sonam Yadav, M.S.
- Aaron Lopez Gonzalez, B.S.
- Gabriel Ruiz, UG
- Dannisa Ortega, UG
- Meghan Worrell, UG
- Jan Hrabovsky, postdoc
- Atlantis Moses and Jose Marquez

Collaborators:

- University of Nebraska Lincoln: Dr. Mathias Schubert and Dr. Megan Stokey
- University of California at Santa Barbara: Dr. Chris Palmstrøm, Aaron Engel, and Dr. Wilson Parreno.
- Members of the J. A. Woollam Company
- Dr. Hyun-Jung Kim at the National Institute of Aerospace

Funding:

- AFOSR (Grant No. FA9550-24-1-0061)
- AFRL (Grant No. FA9453-23-2-0001)
- NSF (Grant No. DMR-2423992).
- The project was initiated with support from the New Mexico Space Grant Consortium (NMSG) and the SCalable Asymmetric Lifecycle Engagement, SCALE (Grant No. W52P1J-22-9-3009) program.
- The growth of the grey tin samples was supported by ARL (Grants No. W911NF-21-2 0140 and No. W911NF-23-2-0031).

Vita

Planned Publications:

- J. R. Love , C. A. Armenta, A. K. Moses, J. Hrabrovsky, S. Zollner, A. N. Engel, and C. J. Palmstrom, "Infrared ellipsometry measurements of carrier concentrations in doped gray α-tin on InSb and CdTe". (To be submitted: J. Appl. Phys.).

- J. R. Love, S. Zollner, M. Stokey, M. Schubert, "Determining the optical constants for commercially available bulk calcium fluoride using ellipsometry". (To be submitted: Surf. Sci. Spectr.).

Submitted Publications & Collaborations:

- J. Hrabrovsky, J. R. Love , L. Strizik, T. Ishibashi, S. Zollner, and M. Veis, " TeO2-BaO-Bi2O3 tellurite optical glasses II. - Linear and non-linear optical and magneto-optical properties". (Submitted to: Opt. Mater., 2025).

- M. Milosavljevic, R. Carrasco, A. Newell, J. R. Love, S. Zollner, C. Morath, D. Maestas, P. Webster, and S. R. Johnson, "Spectroscopic ellipsometry measurement and analysis of the optical constants of InAs/InAsSb and InGaAs/InAsSb superlattices and their bulk constituents ". (Submitted to: J. Appl. Phys., 2025).

- M. R. Arias, C. A. Armenta, C. Emminger, C. M. Zamarripa, N. S. Samarasingha, J. R. Love, S. Yadav, and S. Zollner, "Temperature dependence of the infrared dielectric function and the direct band gap of InSb from 80 to 725 K", J. Vac. Sci. Technol. B 41, 022203 (2023).

- F. Abadizaman, J. R. Love S. Zollner, "Optical constants of single-crystalline Ni(100) from 77 K to 770 K from ellipsometry measurements", J. Vac. Sci. Technol. A 40, 033202 (2022).

New Mexico State Univeristy Work Experience:

- Graduate Assistant, Physics. May 2024 – present
- Research Assistant, Physics. December 2020 – May 2024
- Supplemental Instruction Facilitator, Chemistry. August 2022 – November 2023

Presentations:

- 10th International Conference on Spectroscopic Ellipsometry, Boulder, CO (2025).
- 50th Conference on the Physics and Chemistry of Surfaces and Interfaces, Kailua-Kona, Hawaii,
- AVS 70th International Symposium and Exhibition, Tampa, FL (2024).
- 7th Tri-Service Workshop on GeSn and GeSiSn, Colorado Springs, CO (2024).
- NMSU URCAS, Las Cruces, NM (2022).
- AVS 68th International Symposium and Exhibition, Pittsburg, PA (2022).
- APS March Meeting, Chicago, IL (2022).

Scholarships and Awards:

- NMSGC
- SCALE-RH
- Robert Wichert Award in Creative Writing
- 2021 Zozobra Student T-Shirt Contest

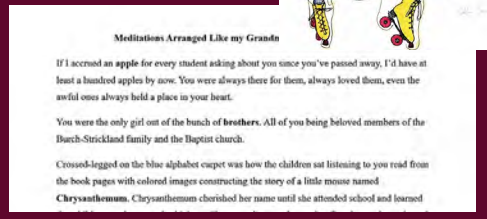
Meditations Arranged Like my Grandn

If I accrued an **apple** for every student asking about you since you've passed away, I'd have at least a hundred apples by now. You were always there for them, always loved them, even the awful ones always held a place in your heart.

You were the only girl out of the bunch of **brothers**. All of you being beloved members of the Burch-Strickland family and the Baptist church.

Crossed-legged on the blue alphabet carpet was how the children sat listening to you read from the book pages with colored images constructing the story of a little mouse named **Chrysanthemum**. Chrysanthemum cherished her name until she attended school and learned

Outline

1. Experimental methods and instrumentation
2. Calcium Fluoride
   - Motivation and sample descriptions
   - Acquisition parameters
   - Infrared SE
   - Visible and VUV SE
   - Summary

3. Grey Tin
   - Motivation
   - Sample descriptions and HRXRD
   - Infrared SE
   - Temperature dependent ellipsometry
   - Optical sum rules: the f-sum rule
   - Experimental data
   - Basis spline polynomial
   - Results
   - Summary

X-Ray Diffraction

→ Empyrean x-ray diffractometer, Malvern PANalytical.

Powder x-ray diffraction optics:

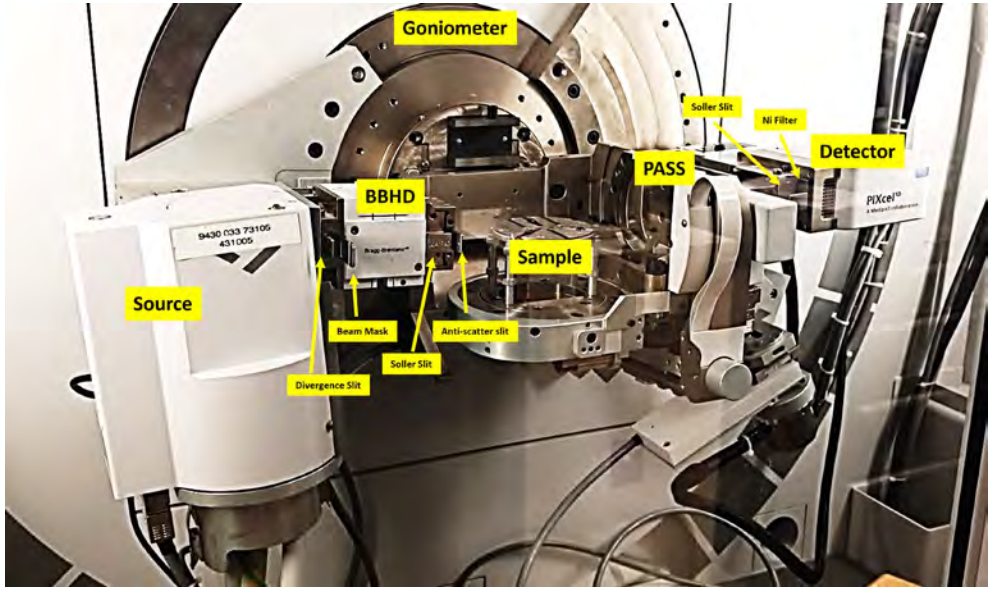

$$2d\sin(\theta) = n\lambda$$

$$d_{hkl} = \frac{a}{\sqrt{h^2 + k^2 + l^2}}$$

$$t = \frac{\lambda}{\Delta\theta_f * 2 * \cos(\theta_L)}$$

- Scans over wide 2θ range
- Lattice constants and surface orientation.
- Continuous x-ray source with characteristic spectral lines: Cu-Ka, Cu-Kb, Cu-L, W

High resolution x-ray diffraction optics:

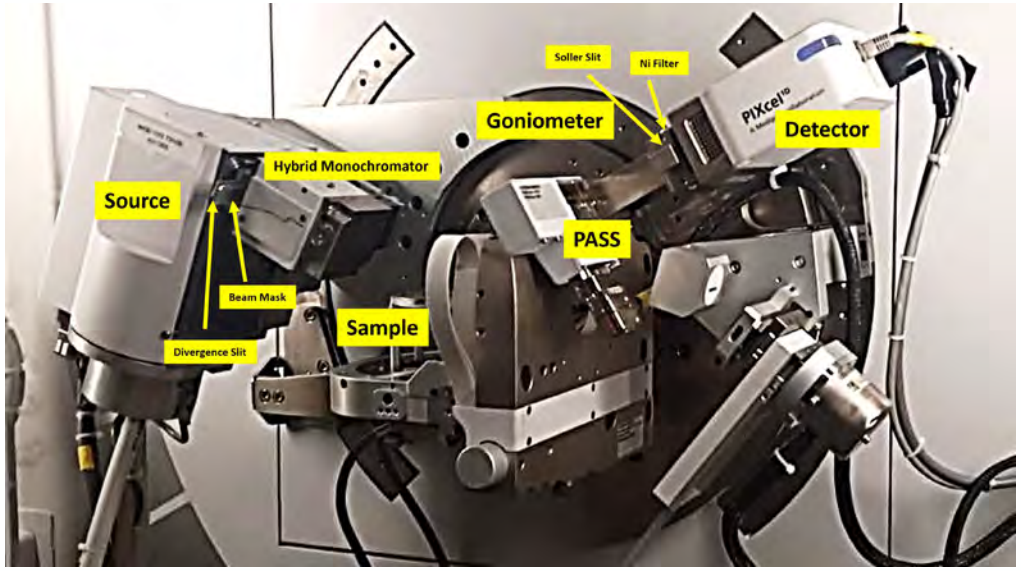

- Scans over short 2θ-ω range → sensitive to thin films.
- Requires an extensive alignment procedure with specific geometry.
- Monochromatic x-ray source: Cu-Ka
- Diffraction pattern shows oscillations, “fringes”, and a simulation of the pattern determines the layer thickness.

SPECTROSCOPIC ELLIPSOMETRY (SE)

$$\rho = \tan(\Psi)e^{i\Delta}$$

$$\langle\epsilon\rangle = \sin^2(\theta_i)[1 + \tan^2(\theta_i)(\frac{1-\rho}{1+\rho})^2]$$

SE measures the change in EM wave polarization after reflection at an interface.

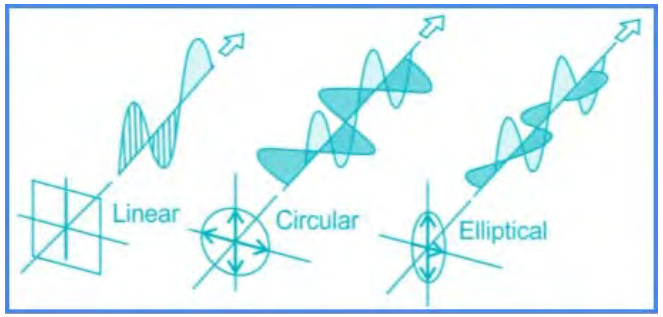

The ellipsometric angles Ψ and Δ represent the amplitude and phase difference between s and p polarization states.

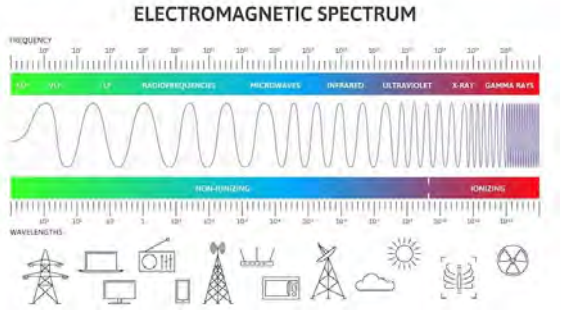

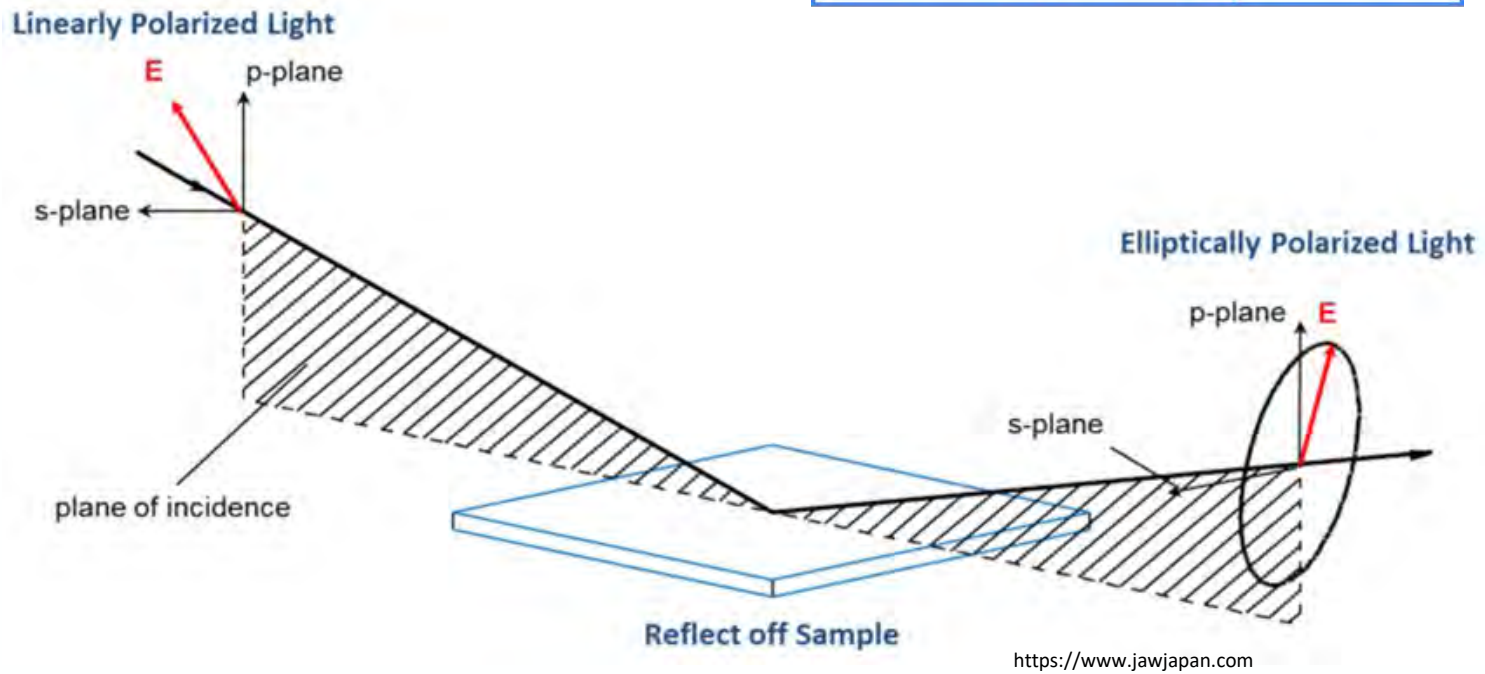

https://www.jawjapan.com

TEMPERATURE DEPENDENT INFRARED ELLIPSOMETRY

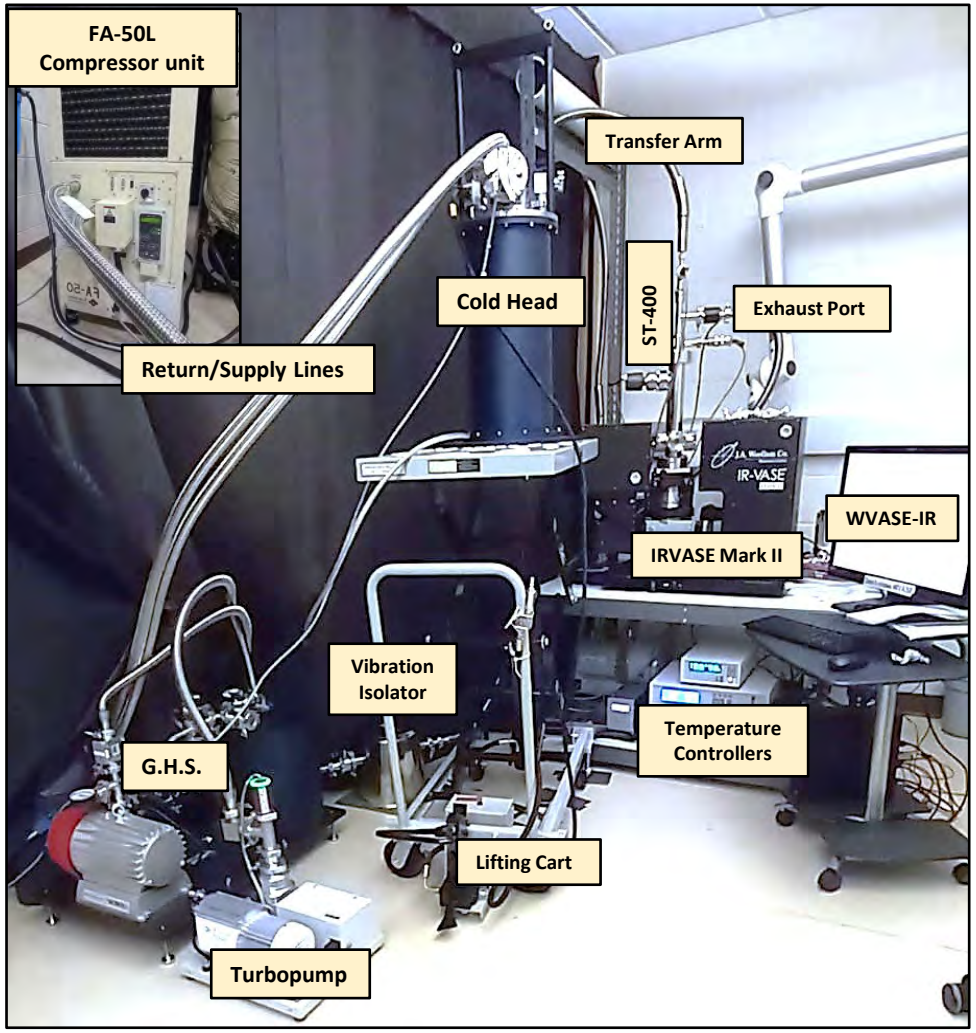

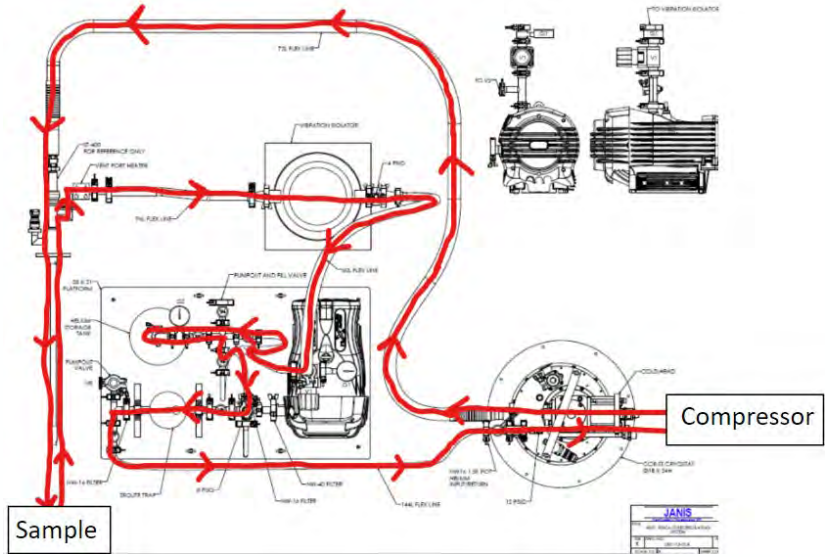

Combined System for Temperature Dependent SE	
FA-50L Helium Compressor Unit	Sumitomo Heavy Industries, Ltd.
RGC4 Cryogen Free Recirculating Gas Cooler	Lake Shore Cryotronics, Inc.
ST-400 Cryostat	Lake Shore Cryotronics, Inc.
IR-VASE Mark II	J.A. Woollam Co.

Joule-Thompson effect: Under certain conditions gasses undergoing a pressure reduction experience a drop in temperature

Cryocoolers are devices that generate a net decrease in the temperature of a gas by mechanically creating such conditions.

There are 3 phases for cooldown:

1. Evacuation of the gas handling system
2. Room temperature He circulation
3. Final cooldown of the sample.

ARO (W911NF-22-2-0130)

CALCIUM FLUORIDE

Refining previously established optical constants for commercially available bulk substrates.

CALCIUM FLUORIDE, CaF_2

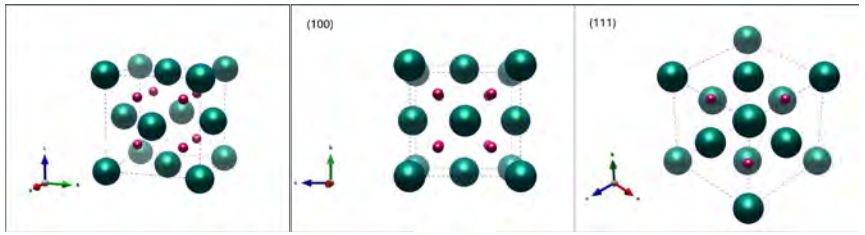

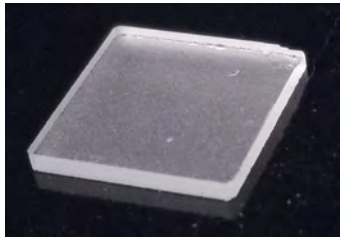

- CaF_2 was used as a substrate for PCM materials with the goal of developing tunable imaging systems for satellites (Dr. H. Kim).

→ The substrate required characterization and commercial CaF_2 wafers were purchased for comparison.

- MTI Corporation grows bulk CaF_2 wafers by Czochralski (CZ) method

1 Single side and 1 double side polished, **10 mm x 10 mm (100) substrates**

1 Single side and 1 double side polished, **10 mm x 10 mm (111) substrates**

- CaF_2 is an insulator with an ultrawide transparency range and large absorption gap of ~11 eV (tomiki, ??). → ideal for use in optical components
- Crystal quality is of high importance for optical components.
- Crystal growth methods have improved.
- Here we evaluate the properties of current commercially available bulk CaF_2 substrates.

Calcium Fluoride Unit Cell	
Formula unit:	CaF_2
Space group:	$Fm\bar{3}m$ (no. 225)
Cell dimensions:	a = 5.4626 Å (Rohrer, ??)
Cell contents:	4 formula units per cell
Atomic positions:	Ca in (4a) $m\bar{3}m$ (0,0,0) +FCC F in (8c) $\bar{4}3m$ (¼, ¼, ¾); (¼, ¼, ¼) +FCC

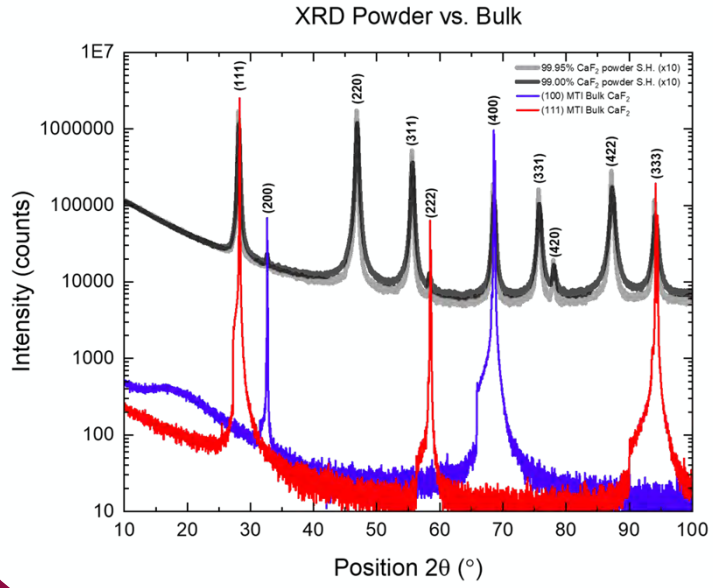

$$2d\sin(\theta) = n\lambda$$

$$d_{hkl} = \frac{a}{\sqrt{h^2 + k^2 + l^2}}$$

$a_{(100)}$ = 5.4778 Å
$a_{(111)}$ = 5.4639 Å

Measurement Conditions

Infrared SE: 1sp (100) and (111) substrates

- Ambient conditions
- Angles of incidence 50°, 60°, and 70°
- 2 cm^{-1} resolution → best signal to noise ratio
- 1 measurement cycle, zone average polarizer and analyzer, 50 scans per compensator position (15).
- Range: 0.01 eV – 0.8 eV

→ Fine step size (resolution) is required to resolve sharp TO phonon peak.

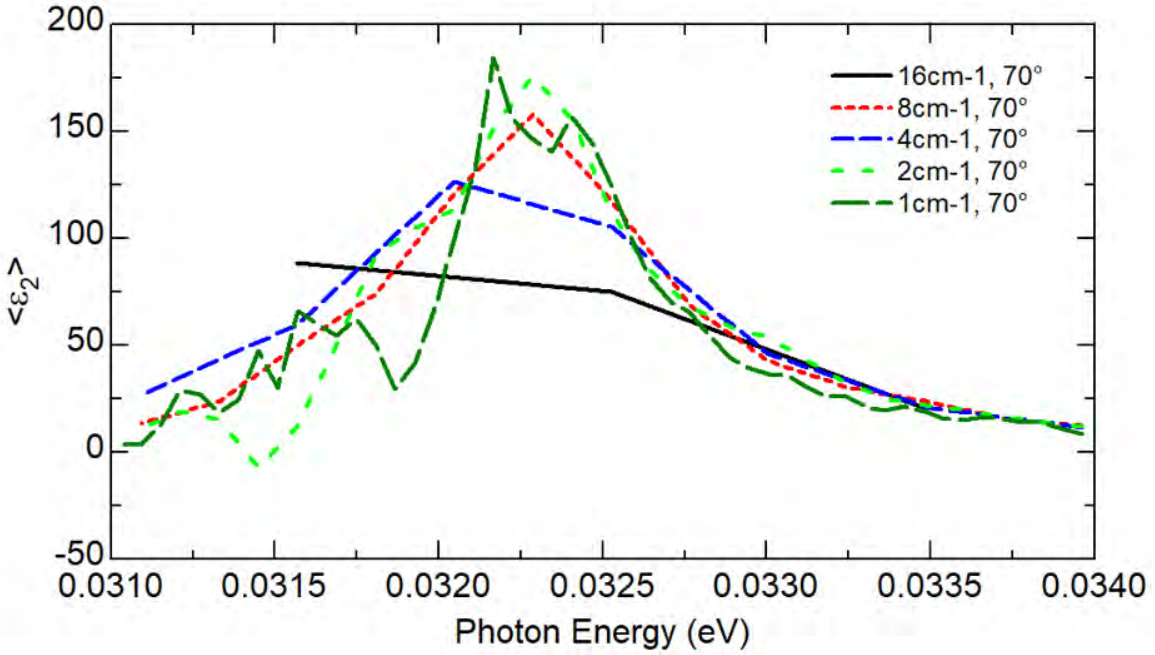

VUV SE: 1sp (100) and (111) substrates

- Room temperature, purged atmosphere
- Angles of incidence 50°, 60°, and 70°
- 1 measurement cycle, zone average polarizer and analyzer, 10 revolutions per measurement.
- Range: 0.5 – 9 eV

→ Transparent region of the material has no sharp features to resolve.

Depolarization for 1sp and 2sp substrates:

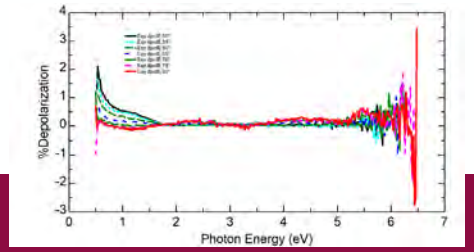

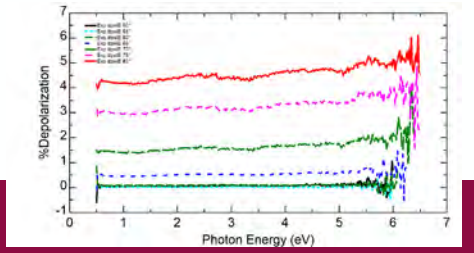

Infrared Ellipsometry

- The restrahlen band (a region of high reflectivity) occurs between the TO and LO phonon modes.

→ Observed as a plateau in Ψ

→ LO is the low energy mode and TO is the high energy mode

→ Larger ionicity = wider band

- More sensitive to small absorption features in this region → multi-phonon absorption

→ The dip at 33 microns is attributed to two phonon absorption [1].

The restrahlen band was modeled with two Lorentzian oscillators:

→ The first is a standard Lorentzian describing the TO phonon mode.

→ The second is an anharmonically broadened Lorentzian used to describe the dip caused by two phonon absorption.

$$\epsilon(\omega) = 1 + \frac{\omega_P^2}{(\omega_0^2 - \omega^2) + i\gamma\omega}$$

	(100)	(111)	HOC.II
ϵ_∞	1.991 ± 0.001	1.973 ± 0.001	2.045
A_{TO}	4.418 ± 0.029	4.161 ± 0.021	
ϵ_s	6.409 ± 0.001	6.134 ± 0.001	
ω_{TO} [cm^{-1}]	259.2 ± 0.249	260.5 ± 0.160	257
Γ_{TO} [cm^{-1}]	4.198 ± 0.465	4.001 ± 0.294	
ω_{2ph} [cm^{-1}]	333.7 ± 1.490	330.99 ± 1.640	328
Γ_{2ph} [cm^{-1}]	75.53 ± 3.560	103.1 ± 2.640	
C_{2ph} [cm^{-1}]	0.289 ± 0.025	0.121 ± 0.121	

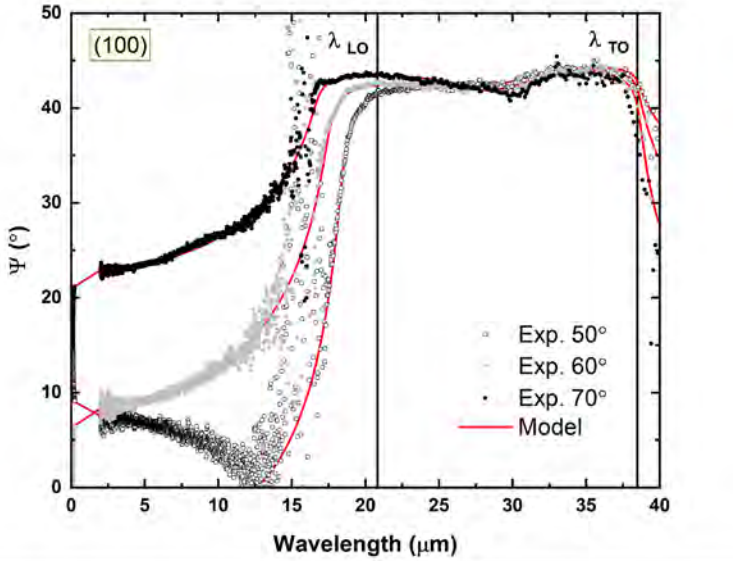

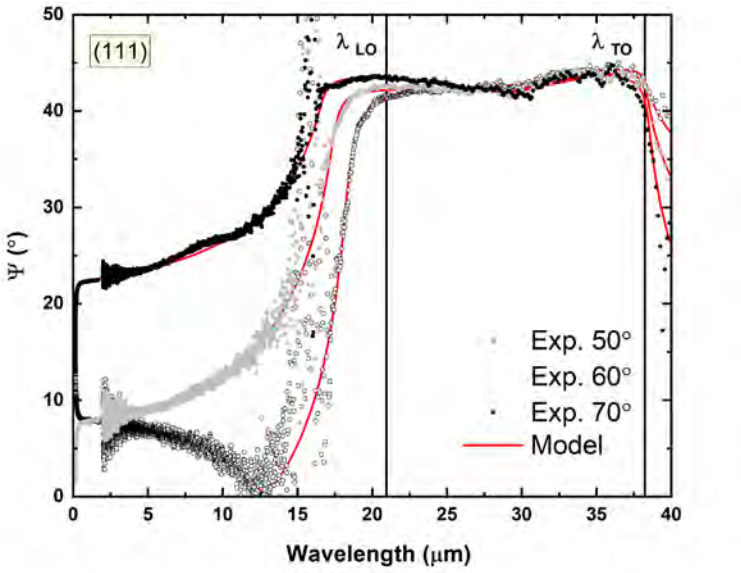

[1] D. F. Bezuidenhout. Handbook of Optical Constants of Solids II. Academic Press, San Diego, 1997, p. 815.

Infrared Active Phonon Modes

Phonons: lattice vibrations

Calcium fluoride has one infrared active phonon mode and one Raman active phonon mode [9, 29].

- The IR active phonon mode splits into one transverse optical (TO) and one longitudinal optical (LO) phonon.
- The TO phonon mode is directly observable as a sharp peak in ϵ_2
- The LO phonon mode is seen in the imaginary part of the loss function [30].
- The high frequency dielectric constant is related to the static dielectric constant through the Lydanne-Sachs-Teller (LST) relationship [30].

$$\epsilon = \epsilon_\infty + \frac{A\omega_{TO}^2}{\omega_{TO}^2 - \omega^2 - i\omega\Gamma_{TO}^2} \qquad \epsilon^- = \epsilon_\infty^- + \frac{B\omega_{LO}^2}{\omega_{LO}^2 - \omega^2 - i\omega\Gamma_{LO}^2}$$

$$\epsilon_s = \epsilon_\infty + A_{TO}$$

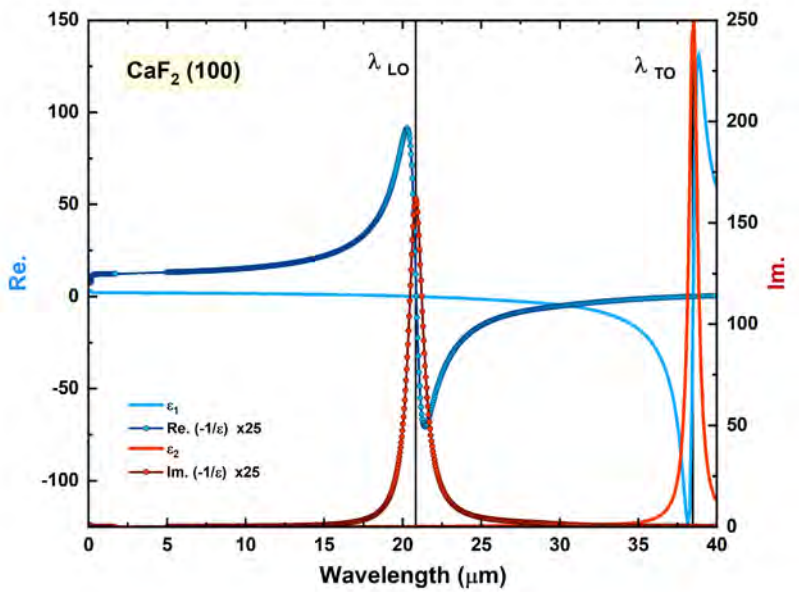

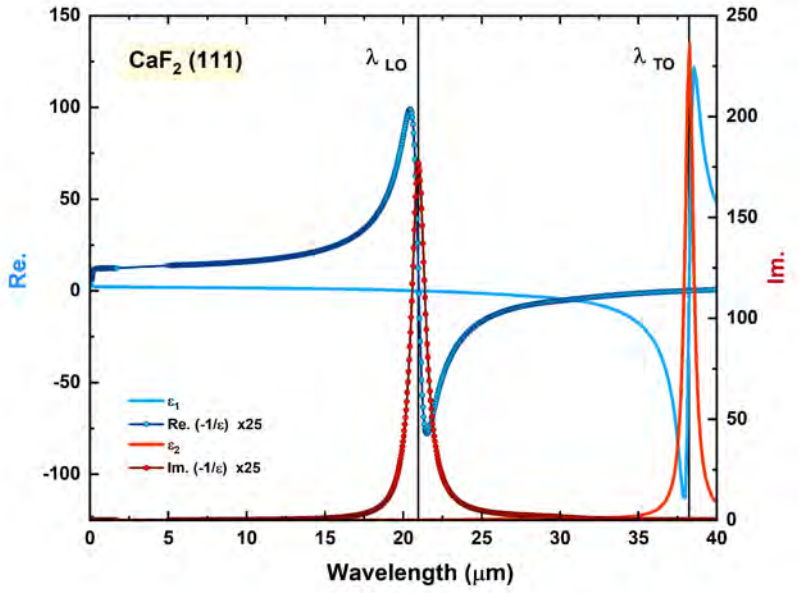

[9] W. Kaiser et al. Phys. Rev. 127 (1962), p. 6.
[29] M. M. Elcombe and A. W. Pryor. J. Phys. C: Solid State Phys. 3 (1970), p. 492.
[30] M. Schubert. Infrared Ellipsometry on Semiconductor Layer Structures Phonons, Plasmons, and Polaritons. Springer-Verlag, Berlin Heidelberg, 2004.

Visible and VUV Ellipsometry

- CaF_2 is transparent in the visible region → no absorption until 11 eV
- The substrate model uses a UV pole and 2 Gaussian oscillators to describe the onset of absorption above 9 eV.
- A surface layer was added to account for the small negative values appearing in $\langle \epsilon_2 \rangle$ above 3 eV.
- A point-by-point fit was done to obtain the dielectric function. → forced ϵ_2 positive, fixed layer thickness

The substrate model may appear redundant but:

Using only the pole above 15 eV to describe the absorption leaves the MSE larger than 7 for the overall fit, but if the second Gaussian is included near 9.5 eV then the MSE is closer to 3.5.

Comparison with the Handbook of Optical Constants of Solids II (HOC):

- HOC tabulated the complex refractive index of CaF_2 from 2 meV to 41 eV.
- Experimental data in the transparent region agrees well will with literature values.

→ Sharper rise in ϵ_1 above 8 eV for (111)

→ Both substrates show an early absorption onset relative to the literature.

-	(100)	(111)
A_{pole}	224.1 ± 2.390	261.0 ± 6.030
E_{pole} [eV]	15.35 ± 0.208	17.62 ± 0.327
A_1	0.993 ± 0.104	0.042 ± 0.009
E_1 [eV]	7.344 ± 0.114	7.593 ± 0.040
Γ_1 [eV]	2.895 ± 0.137	0.442 ± 0.109
A_2	0.904 ± 0.081	3.523 ± 0.152
E_2 [eV]	9.459 ± 0.104	9.560 ± 0.050
Γ_2 [eV]	1.159 ± 0.010	0.775 ± 0.053

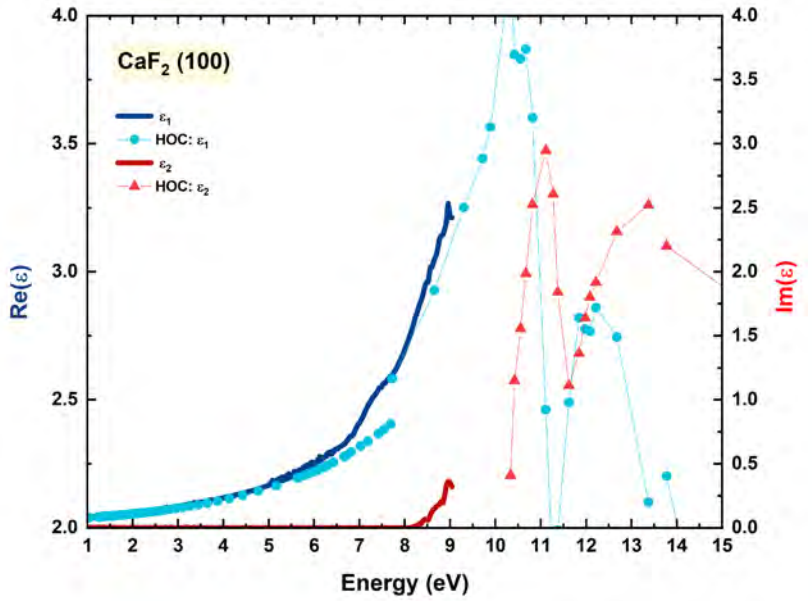

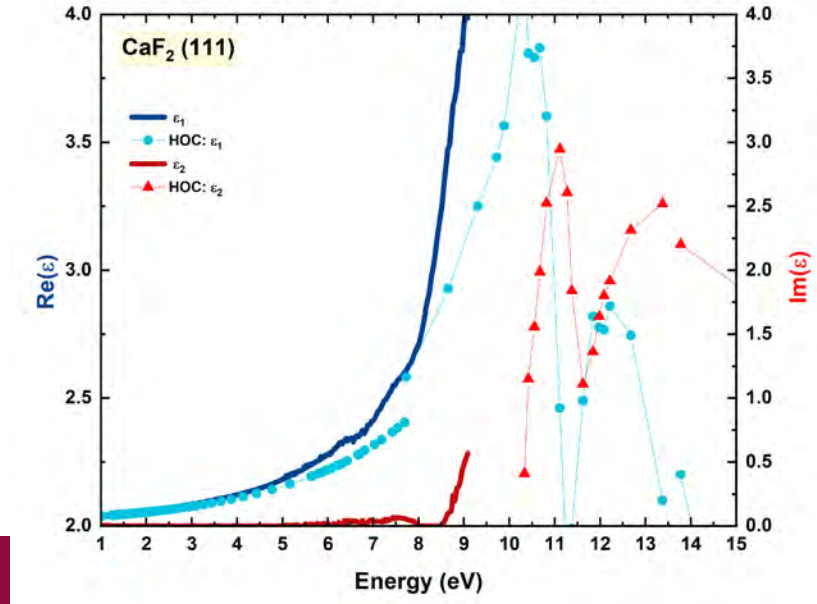

[1] D. F. Bezuidenhout. Handbook of Optical Constants of Solids II. Academic Press, San Diego, 1997, p. 815.

Lattice Defects and Color Centers

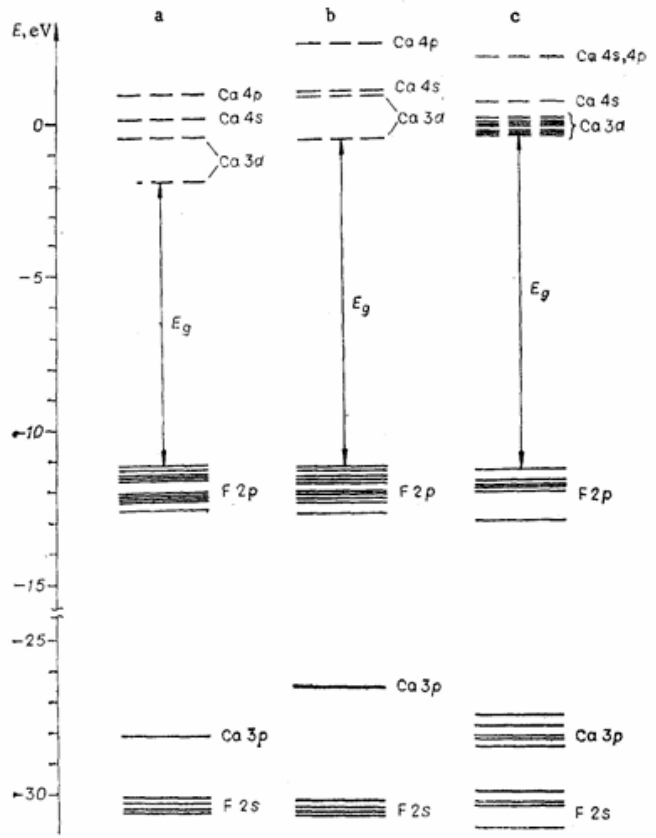

Fig. 1. Comparison of energy diagrams for various clusters in CaF_2: a) free $[CaF_8]^{6-}$ cluster; b) $[CaF_8]^{6-}$ in the pseudopotential of four spheres of neighbors; c) the $[Ca_4F_7]^{1+}$ system in the pseudopotential of nine coordination spheres from the data of [13].

- Defects that arise from the crystal growth process are identified as oxygen ions filling in for fluorine vacancies, “color centers” [41].
- It was shown that contamination by oxygen ions or hydroxyl ions causes the onset of absorption to decrease in the visible and VUV spectra.
- The influence of defects was studied by comparing band energy diagrams for a perfect CaF_2 lattice and ones that contain impurities [4].
- When there is a single vacancy in the CaF_2 cell the 2p fluorine band narrows and the calcium 3d band splits into three levels.
- This splitting causes absorption edge to decrease to 7 eV.

[4] N. I. Medvedeva et al. Plenum Publishing Corporation, 1985, p. 649.
[41] P. Feltham and I. Andrews. Phys. Stat. Sol. 10 (1965), p. 203.
[10] T. Tomiki and T. Miyata. J. Phys. Soc. Jpn. 27 (1969), p. 658.

Surface Layer Discussion

- There is very small negative pseudo-absorption between 3.5 and 8.5 eV. → non-physical feature
- The feature appears in both samples.
- Suspected the presence of a surface layer with a larger refractive index than the bulk substrate.
- Added the surface layer and fit the layer thickness → the MSE was reduced appreciably from 3.5 to 3.
- For the point-by-point fit the value of ϵ_2 is fixed positive.

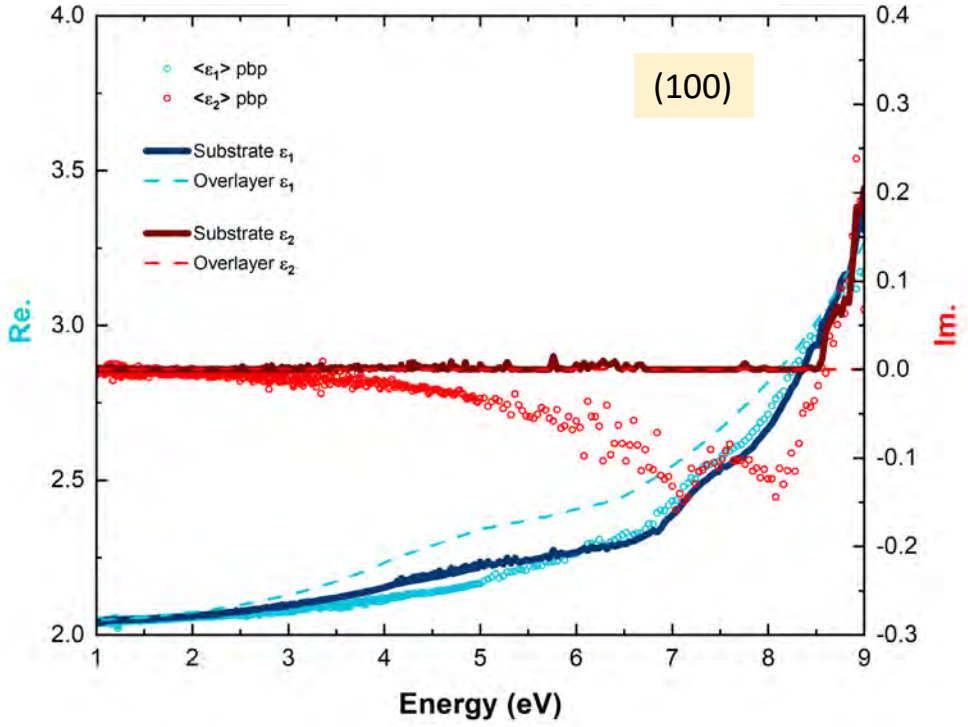

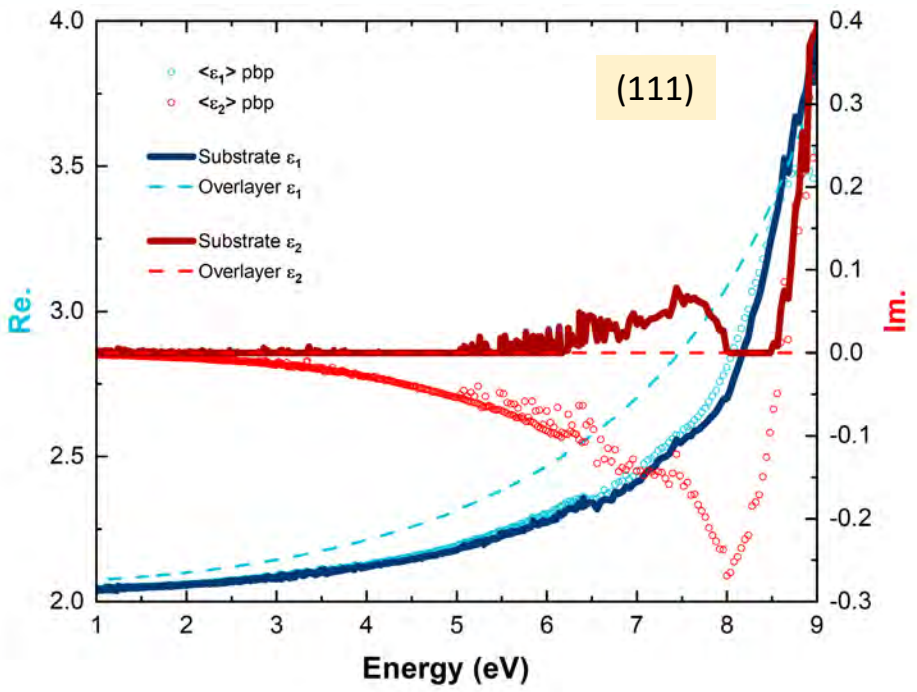

Deviation of the TO Phonon Mode

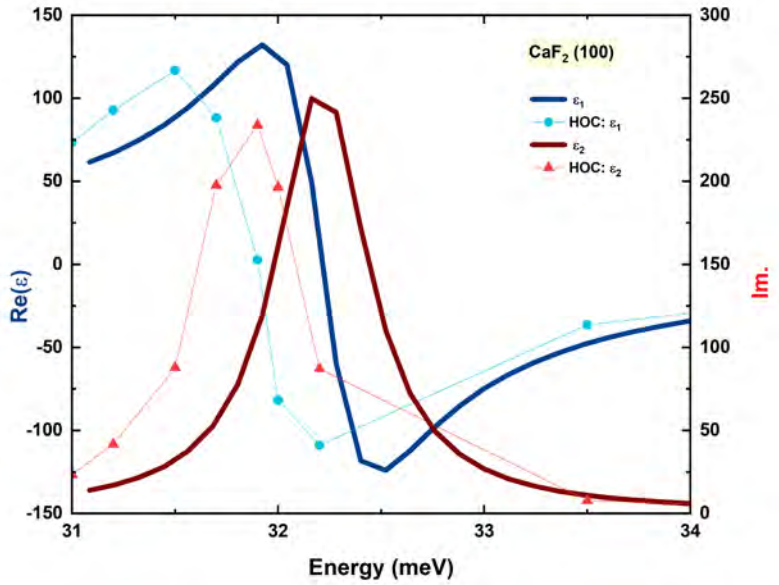

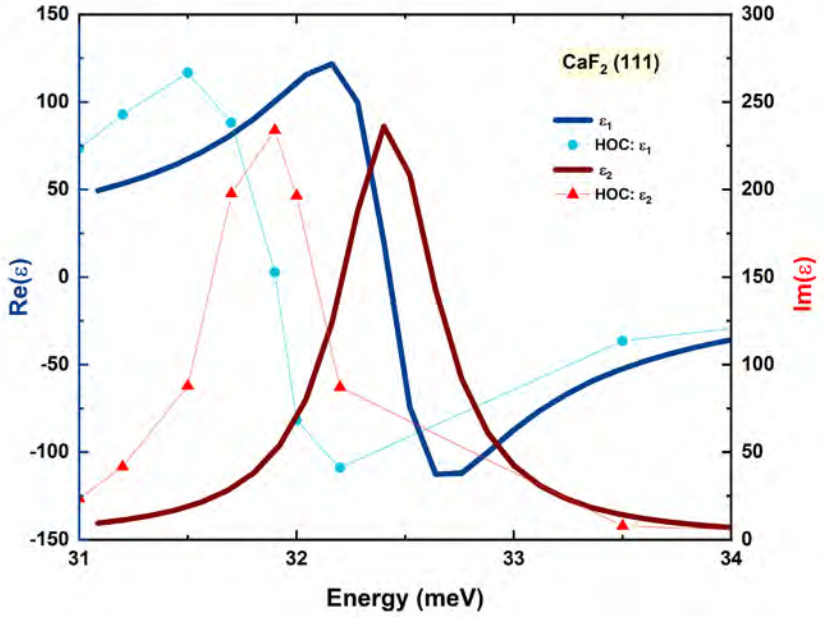

$$\epsilon = \epsilon_\infty + \frac{A\omega_{TO}^2}{\omega_{TO}^2 - \omega^2 - i\omega\Gamma_{TO}^2}$$

- Comparison of the TO phonon mode with HOC shows a deviation in the mode frequency

→ The MTI CaF2 (100) has the mode frequency appearing about 0.5 meV above the literature values.

→ The MTI CaF2 (111) has the mode frequency mode appearing about 1 meV above the literature values.

Was the temperature the same for both samples? → yes, ambient conditions and ~ 24◦ C [8]

What else is different?

- The VUV model found that the (111) sample has a thicker overlayer than the (100) sample.
- There is a sharper rise in ϵ_1 when approaching the absorption edge for (111) than for (100)

Could it be defects?

→ The mode frequency is related to bond strength between the basis atoms.

→ The lattice constants vary slightly between the (100) and (111)

Is it significant?

Summary

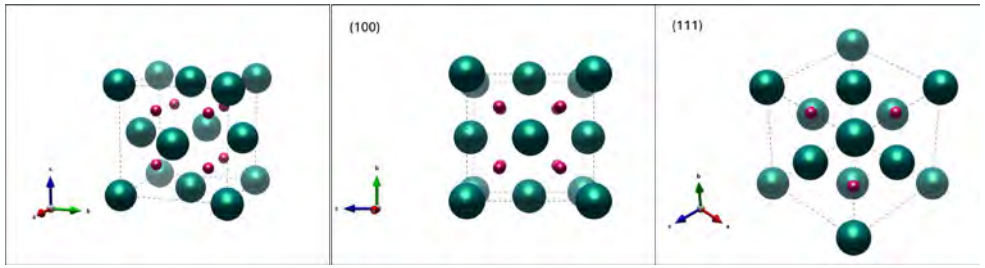

- Confirmed surface orientations and lattice constants

$a_{(100)}$ = 5.4778 Å

$a_{(111)}$ = 5.4639 Å

a = 5.4626 Å

- Identified restrahlen band and infrared active phonon modes

→high reflectivity region is sensitive to two phonon absorption processes

- Measured visible ellipsometry spectra up to 9 eV

→ Good agreement with literature up to absorption edge onset

→ Color centers decrease the absorption onset

→ VUV SE is sensitive to thin films, and the model is improved by adding a surface layer

- Comparison with literature shows good agreement

→ Deviations in TO phonon mode frequency

→ The onset of absorption is lower than expected, (especially for (111))

→ color centers, defects

-	(100)	(111)
A_{pole}	224.1 ± 2.390	261.0 ± 6.030
E_{pole} [eV]	15.35 ± 0.208	17.62 ± 0.327
A_1	0.993 ± 0.104	0.042 ± 0.009
E_1 [eV]	7.344 ± 0.114	7.593 ± 0.040
Γ_1 [eV]	2.895 ± 0.137	0.442 ± 0.109
A_2	0.904 ± 0.081	3.523 ± 0.152
E_2 [eV]	9.459 ± 0.104	9.560 ± 0.050
Γ_2 [eV]	1.159 ± 0.010	0.775 ± 0.053

	(100)	(111)	HOC.II
ϵ_∞	1.991 ± 0.001	1.973 ± 0.001	2.045
A_{TO}	4.418 ± 0.029	4.161 ± 0.021	
ϵ_s	6.409 ± 0.001	6.134 ± 0.001	
ω_{TO} [cm^{-1}]	259.2 ± 0.249	260.5 ± 0.160	257
Γ_{TO} [cm^{-1}]	4.198 ± 0.465	4.0012 ± 0.294	
ω_{2ph} [cm^{-1}]	333.7 ± 1.490	330.99 ± 1.640	328
Γ_{2ph} [cm^{-1}]	75.53 ± 3.560	103.1 ± 2.640	
C_{2ph} [cm^{-1}]	0.289 ± 0.025	0.121 ± 0.121	

[41] [4] 10

GREY TIN (α-Sn)

Using the f-sum rule to determine carrier density as a function of temperature for epitaxial thin films.

Low Temperature Phase of Tin: α-Sn

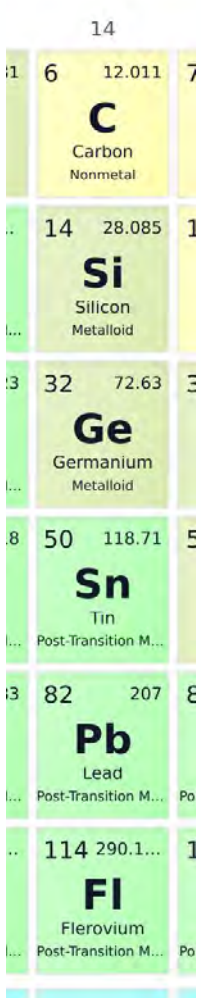

Band structure

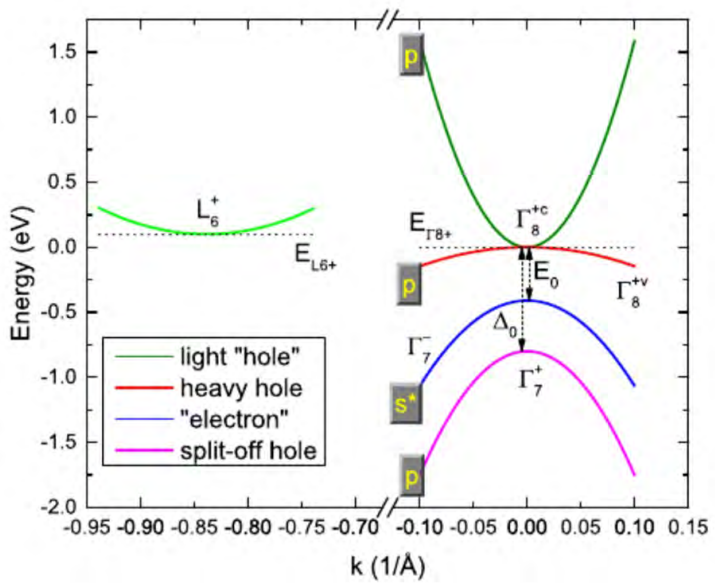

The band structure is tunable by changing the doping, strain, and layer thickness

- α-Sn has an inverted band structure relative to the lighter group IV elements → relativistic effects and the Darwin Shift

Consequently:

- The Γ_8^+ band is degenerate at k = 0 (no lattice strain).
- Γ_8^{+c} has positive curvature (inversion) → Conduction band (CB).
- Γ_7^- has a negative curvature → Valence band (VB).

→ The degeneracy of the Γ_8^+ band makes α-Sn is a gapless semimetal.
→ Intervalence band (IVB) transitions are possible from Γ_7^- into Γ_8^+

The $\overline{E_0}$ transition is observable as an absorption peak in infrared ellipsometry spectra.

R. A. Carrasco, et al., Appl. Phys. Lett. 113, 232104 (2018).
[18] R. A. Carrasco et al. Appl. Phys. Lett. 114 (2018),.

Temperature dependence of

Band structure

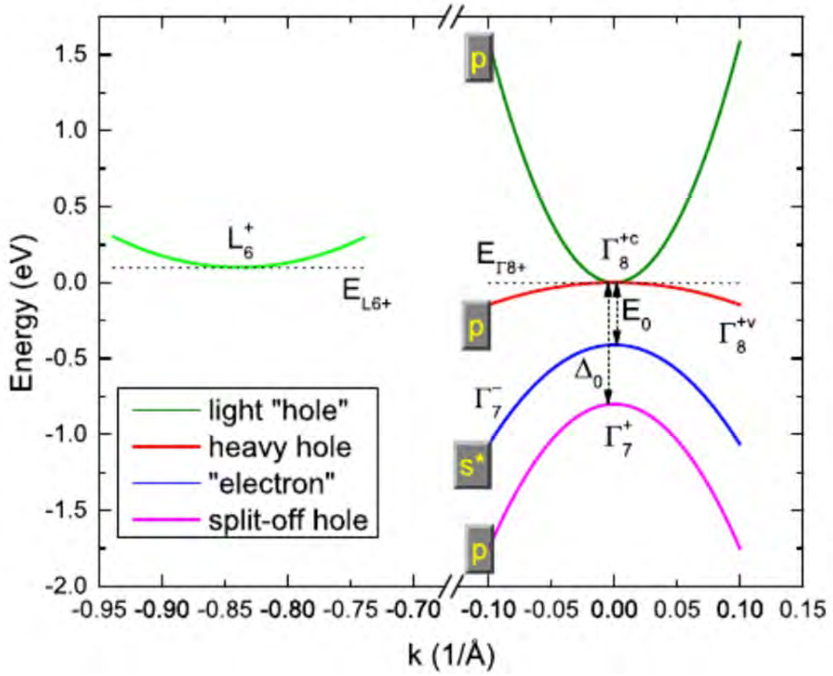

$$f(E) = \frac{1}{\exp\left(\frac{E-\mu}{k_B T}\right) + 1}$$

← The Fermi-Dirac distribution

- The Γ_7^- VB is always fully occupied.
- The chemical potential is lowest at room temperature.
- For intrinsic α-Sn at 0 K the Γ_8^+ is fully occupied → IVB transitions are not allowed

When are they observed?

- Thermal activation
- Doping α-Sn with acceptor ions
- Increasing the number of available states influences the oscillator strength of the $\bar{E}_0$ transition

→ Observed as a change in amplitude for the absorption peak

R. A. Carrasco, et al., Appl. Phys. Lett. 113, 232104 (2018).
S. Zollner, *J. Vac. Sci. Technol. B* 1 , (2024); 42 (2): 022203

Grey Tin

α-Sn
Space Group: F d -3 m (#227-1)
a = 6.48920 Å α = 90.0000°
V = 273.2584 Å^3

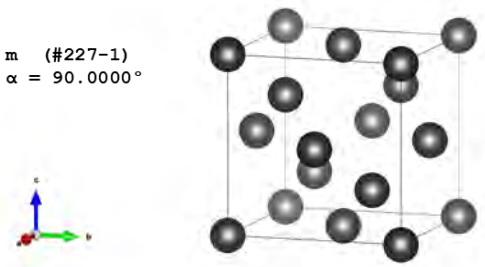

Name	Layers	Growth
AE225	**30 nm α-Sn / InSb (100) c(8x2)**	- **Atomic hydrogen clean at 285°C.** - **Anneal at 360°C.**
AE227	**30 nm α-Sn / InSb (100) c(4x4)**	- **Atomic hydrogen clean at 285°C.** - **Anneal at 430°C under Sb_4 flux.**
RAC InSb	70 nm α-Sn / InSb (100) c(8x2)	- Atomic hydrogen at 200°C.
RAC CdTe	70 nm α-Sn / CdTe (100) c(2x1)	- Slow anneal at 115 ° - RHEED monitors desorption of a-Te

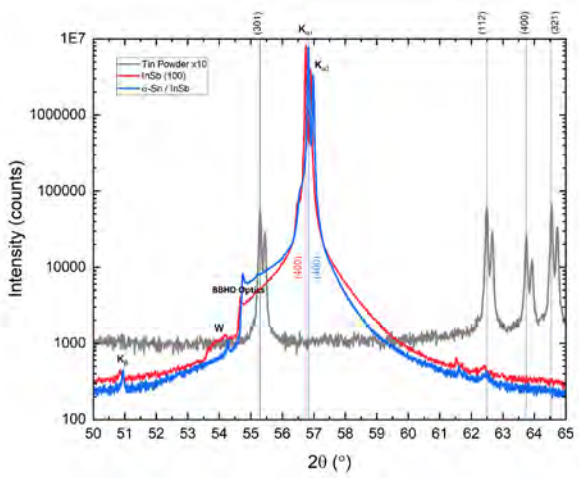

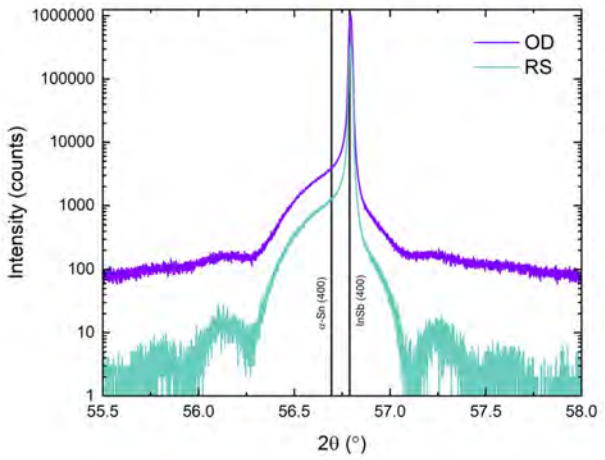

- Collaborators used MBE to grow 30 nm α-Sn layers on InSb (100) substrates with different interface preparations (Engel, ??).
- Results are compared with a previous study of 70 nm α-Sn layers grown using MBE on InSb and CdTe substrates (Carrasco, 2019).

→ The study finds the onset of absorption for $\bar{E}_0$ at 0.41 eV

→ Demonstrates that the strength of the $\overline{E_0}$ absorption peak depends on the substrate material.

PXRD: Comparison of bulk spectra with β-Sn powder spectra.
→ no phase transition

HRXRD: symmetric (004) 2θ-ω scan confirms the 30 nm layer thickness.
→ t = 29.7 ± 0.7 nm

Carrasco, et al., Appl. Phys. Lett. 114, 062102 (2019)
A. N. Engel et al. Phys. Rev. Mater. 8 (2024), p. 044202.

TEMPERATURE DEPENDENT INFRARED ELLIPSOMETRY

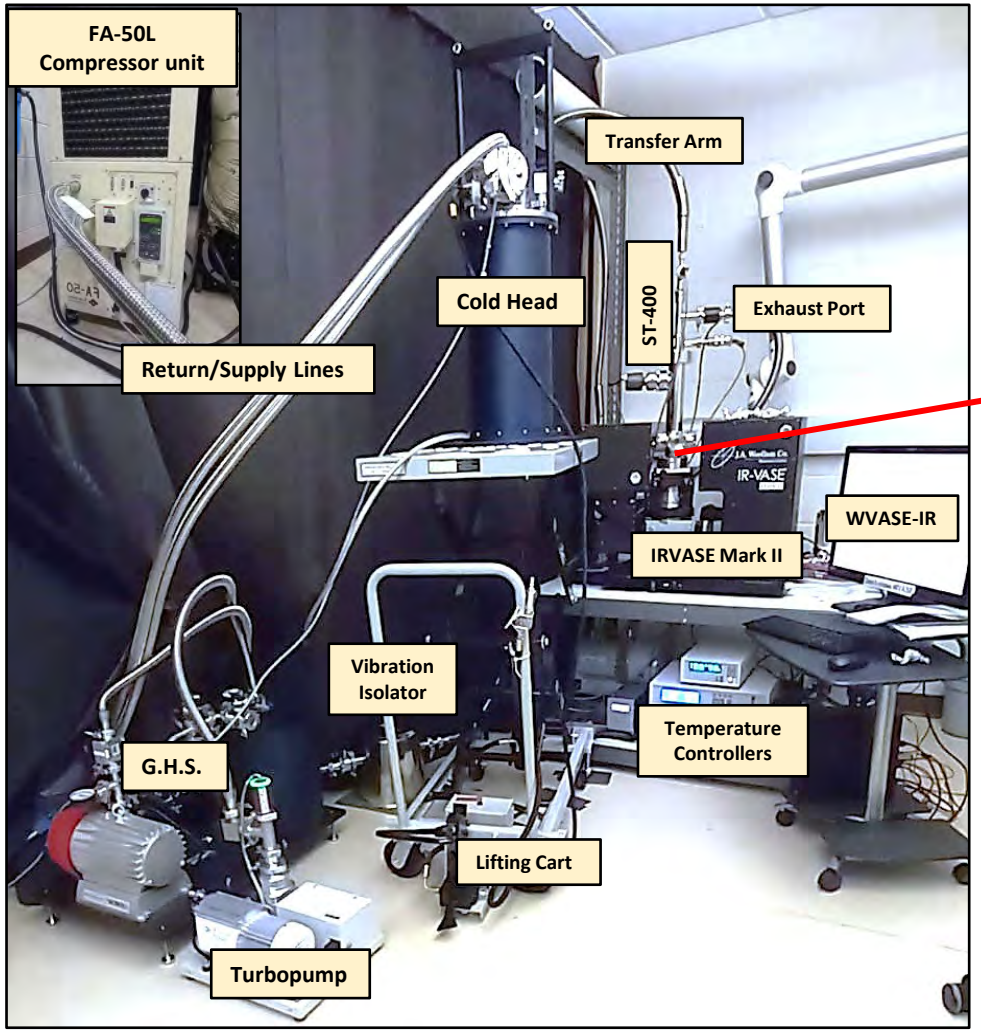

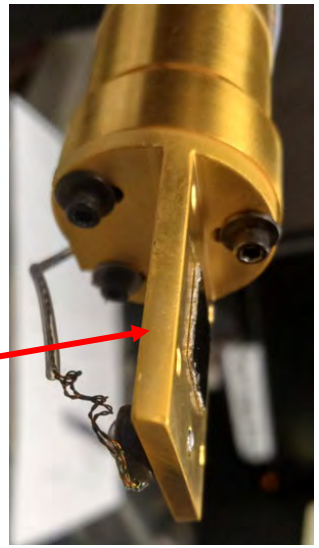

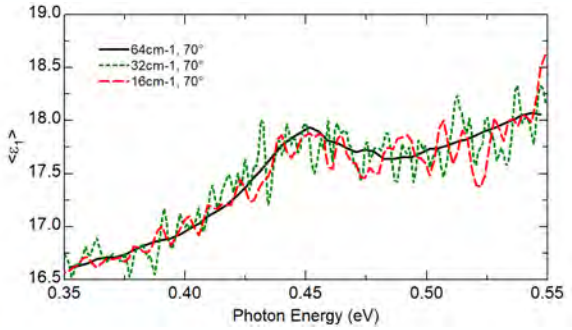

Sample preparation:

- Samples were mounted to the stage using Ag conductive paint.

~~Baking~~ ~~Cleaning~~

- Light pressure with a microfiber cloth to maximize contact and level the surface.
- The Ag paint cured overnight at room temperature.
- Chamber was evacuated over the course of several days to < 1E -8 Torr.

Measurement procedure:

- 300 K scans were taken outside of the cryostat.
- The sample was then aligned inside the cryostat.
- Programed an automated temperature series in WVASE-IR.
- Collected data from 300 K to 10 K in 25 K steps with 64 cm^{-1} resolution.
- 2 measurement cycles and 500 scans per compensator position.

ARO (W911NF-22-2-0130)

Pseudo dielectric function

$$\rho = \tan(\Psi)e^{i\Delta}$$

$$\langle\epsilon\rangle = \sin^2(\theta_i)[1 + \tan^2(\theta_i)(\frac{1-\rho}{1+\rho})^2]$$

- Kramers-Kronig consistency
- E_0 of InSb is seen at 0.17 eV with blueshift towards low temperatures.
- $\bar{E}_0$ of α-Sn has a maximum at 0.45 eV and the amplitude decreases towards low temperatures.

→ B-spline fit of experimental data provides the dielectric function from 300 K – 10 K for the intrinsic and n-type samples.

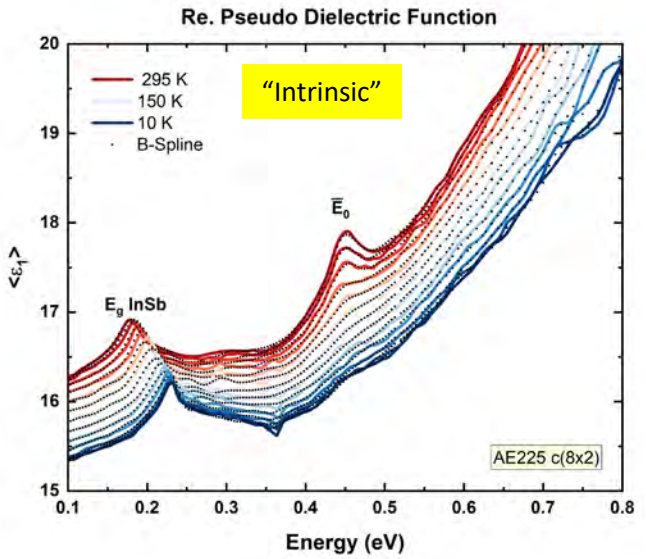

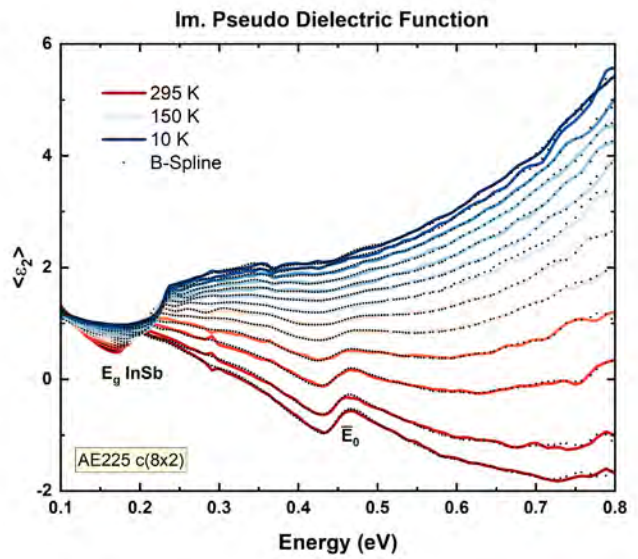

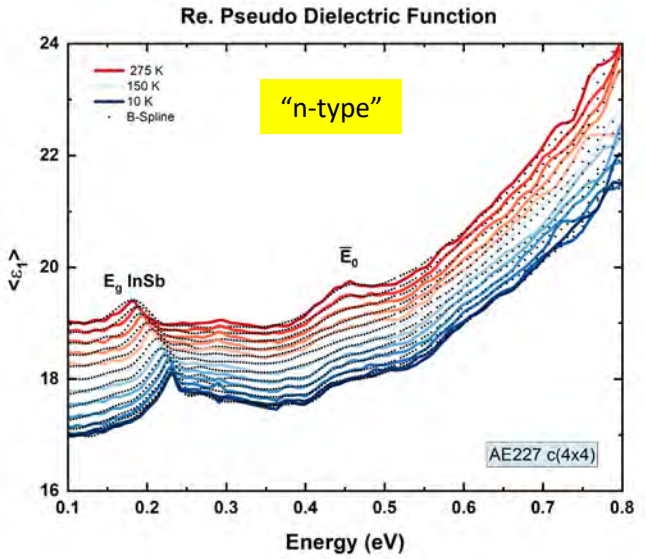

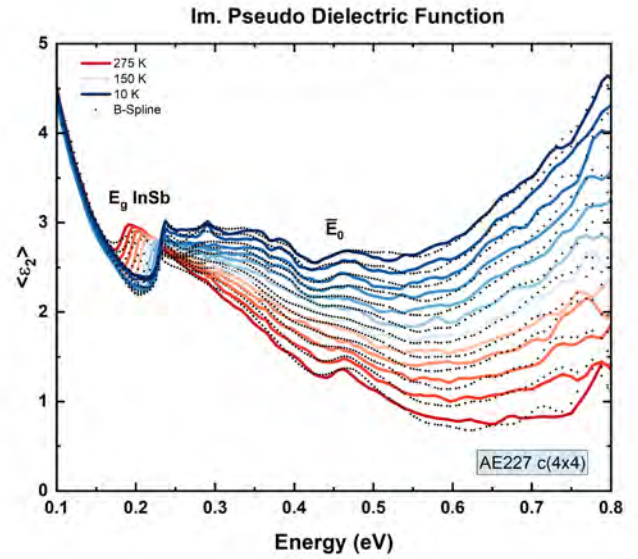

Basis Spline Polynomials

- CompleteEase (CE)
- The b-spline is a summation of basis polynomials whose center positions are localized and separated by a user specified distance (node spacing).
- The result is a smooth curve that follows experimental data and represents the dielectric function.

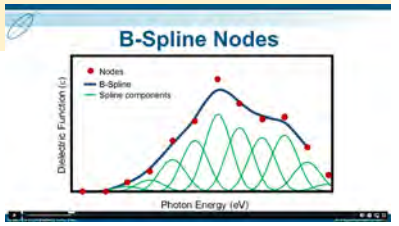

- The substrate optical constants were determined previously down to 77 K

CompleteEase

- Layer # 1 = B-Spline Thickness # 1 = 30.00 nm
  - Resolution (eV) = 0.0200 35 Pts. (0.099-0.796 eV) **Draw Node Graph**
  - Fit Optical Constants = ON
  - Use KK Mode = ON (In Use)
  - **Kramers-Kronig**
    - E Inf = 1.000
    - IR Amp = **0.143** (fit) IR Br = 0.000
    - Use Default Tie Off Behavior = ON
    - View Tie Off Positions = OFF
  - **Nodes**
    - Init. Values: n = 1.500 k = 0.00 Starting Mat. = Gen-Osc
    - Force E2 Positive = ON
    - Assume Transparent Region = OFF
    - Show Nodes = OFF
    - Node Spacing Spectral Ranges: Add Delete Delete All
  - **Advanced**
    - Show Parameters in Fit Results = OFF
    - Pre-Fit When Changing Wavelengths = ON
    - Fix Node Bounds When All Wavelengths Selected = OFF
    - Query Remote System for Optical Constants = OFF

Substrate = PSEMI-E0-InSb_300_tabulated

WVASE

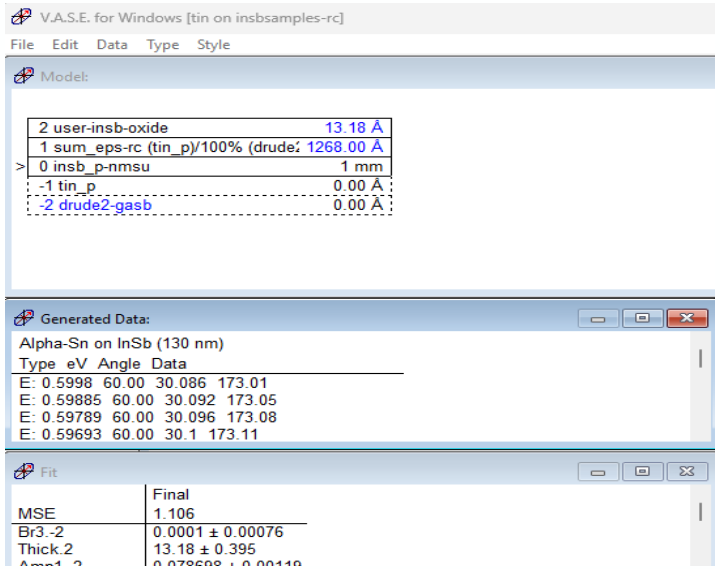

→ Localized positions means that the basis functions are independent of each other.

→ No material reference file is needed.

→ No oscillators need to be placed.

✓ Requires knowing the layer thickness (HRXRD)

✓ Requires knowing the substrate optical constants.

✓ Must choose an appropriate node spacing

✓ Employ Kramers-Kronig consistency and force ϵ_2 positive

[34] J. Mohrmann et alJ. Vac. Sci. Technol. B 38 (2020), p. 014001.

Optical Sums: The f-sum Rule

Thomas-Reich-Kuhn Rule:
The sum of all oscillator strengths for all transitions will equal the total electrons in an atom.

$$\sum_{j'} f_{j'j} = Z$$

Oscillator strength density → f(ω)

Calculated from fundamental constants, frequency and ε_2 this value corresponds to a material with N electrons per volume.

$$f(\omega) = \frac{m}{2\pi^2 e^2}\,\omega\,\mathrm{Im}\epsilon(\omega) \qquad \int_0^\infty f(\omega)\,d\omega = \mathfrak{N}$$

Integration over the oscillator strength density :

$$\int_0^\infty \omega\,\mathrm{Im}\epsilon(\omega)\,d\omega = \tfrac{1}{2}\pi\,\omega_p^2$$

Plasma Frequency → ω_P:

The plasma frequency can then be used to determine electron density N.

$$\omega_p^2 = 4\pi\,\mathfrak{N}e^2/m$$

$$\bar{E}_0 \int_{E_a}^{E_b} \epsilon_2(E)dE = \frac{\pi}{2}\frac{pe^2\hbar^2}{\epsilon_0 m_0 m^*_{hh}}$$

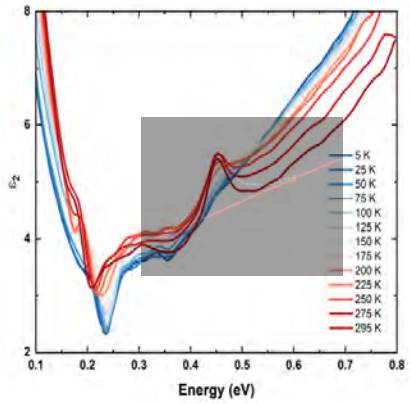

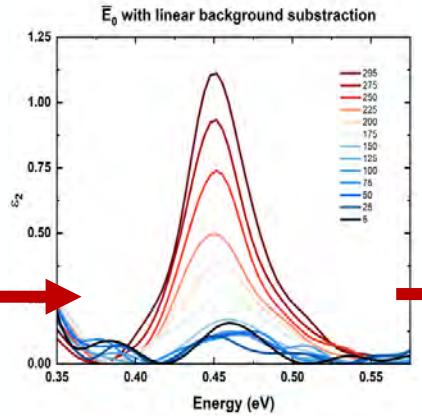

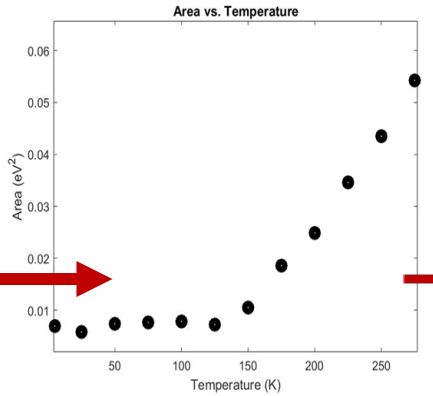

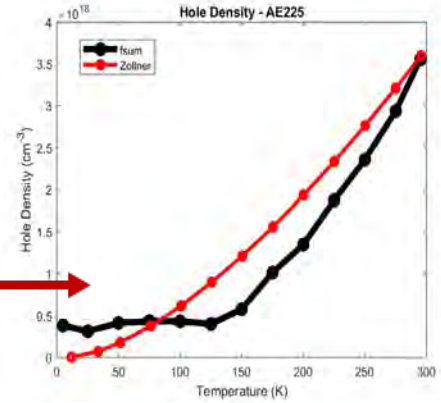

- First a linear background is subtracted to find integrated peak intensity.
- The maximum position gives the greatest contribution and is pulled out of the integral as a constant.
- The heavy hole effective mass (0.26 m_0) is known through magneto-reflectance measurements (Groves, ??).
- Solve for the hole density, p

M. Altarelli, et. Al., Phys. Rev. B, 6(12), 4502–4509 (1972).
F. Abadizaman, et al., *J. Vac. Sci. Technol. B 37(6), (2019).*
S. Zollner, *J. Vac. Sci. Technol. B* 1 , (2024); 42 (2): 022203
S. H. Groves et al. J. Phys. Chem. Solids 31 (1970), p. 2031.

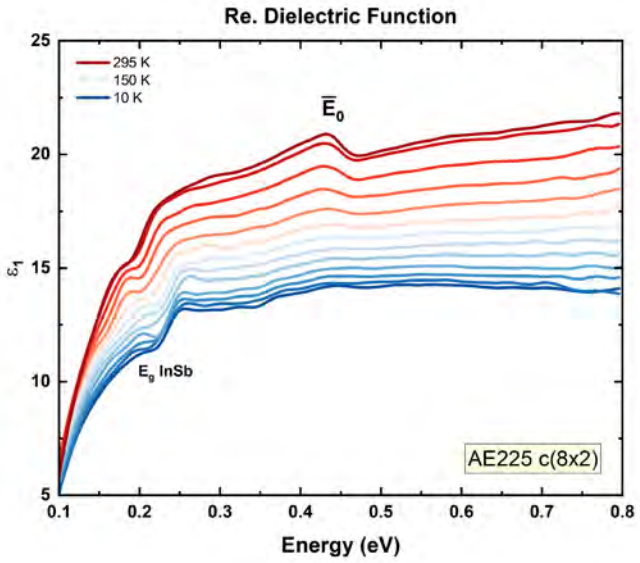

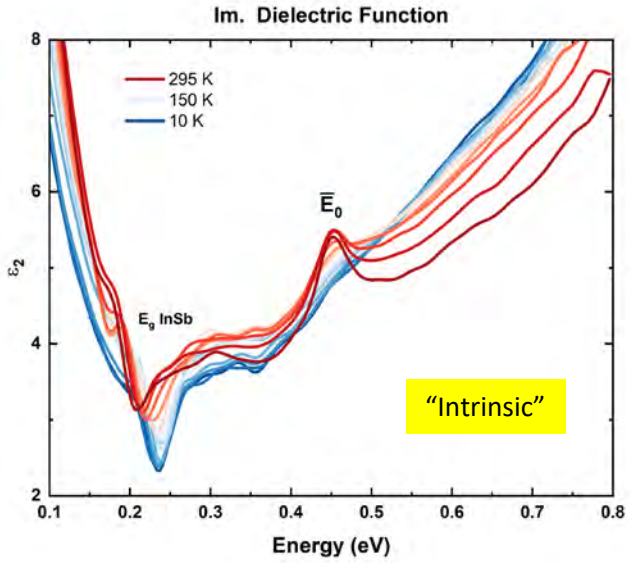

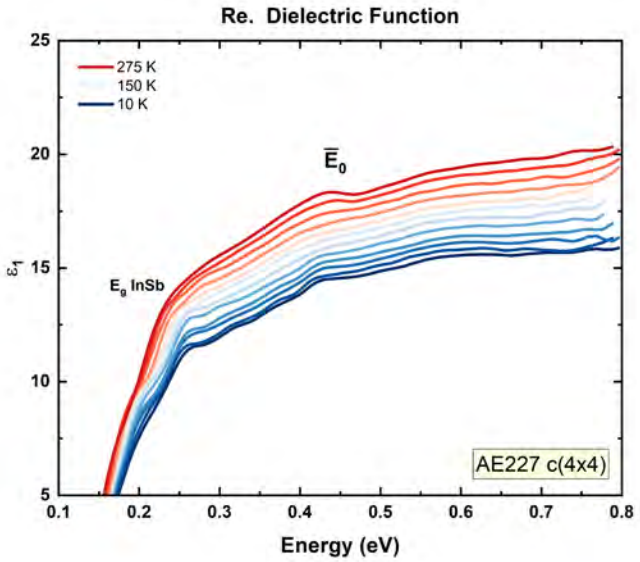

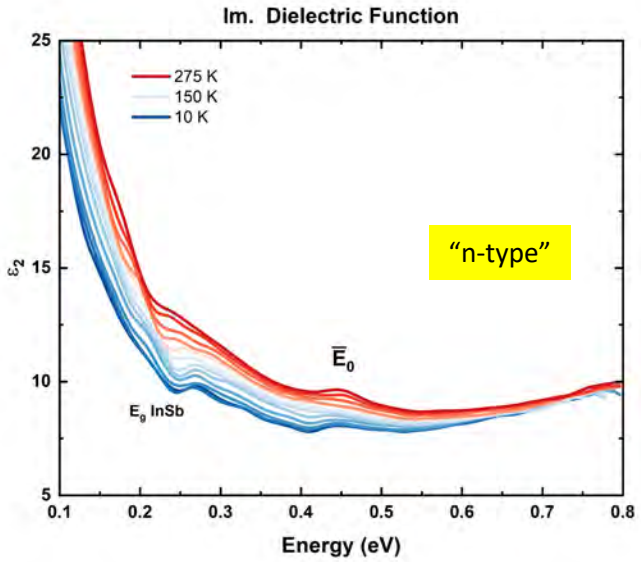

Dielectric Function

- Interference effects from the InSb bandgap near 0.2 eV.
- Square root increase of e1
- Largest amplitude of $\bar{E}_0$ at high temperatures.
- Increasing absorption above 0.3 eV for AE225.
- The slope changes with temperature → suspect ice formation

Linear Background Subtraction

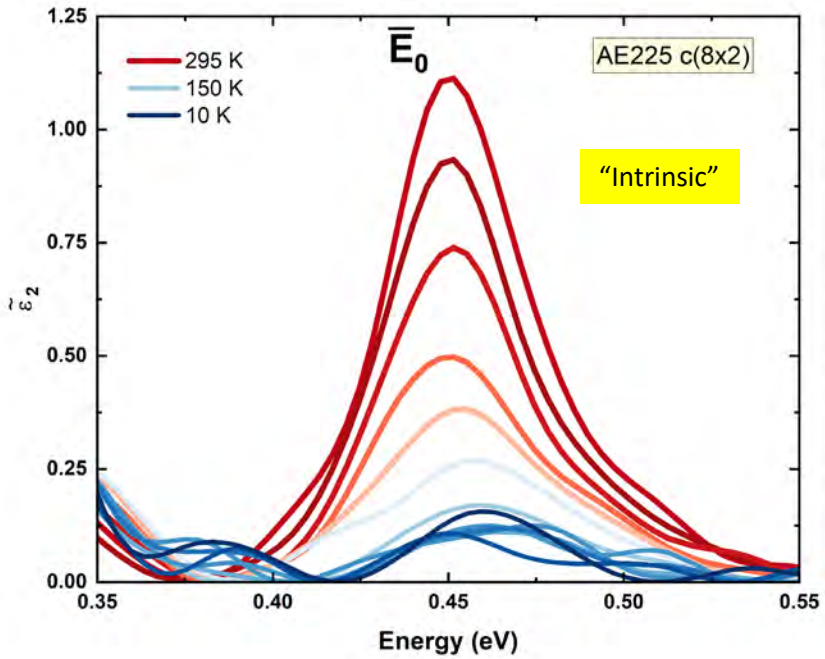

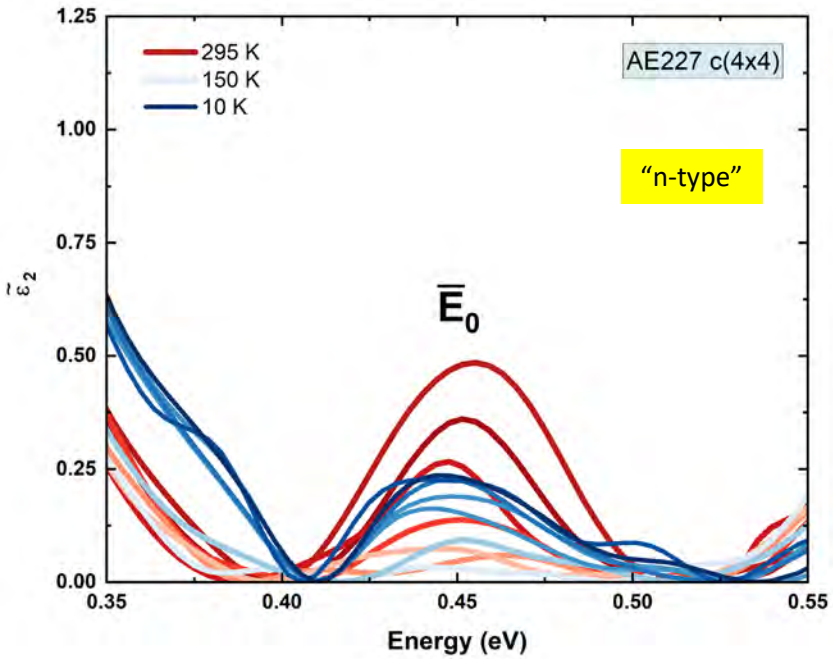

AE225 c(8x2): In rich interface

→ low p-type doping introduces more heavy holes in Γ_8^{+v}

AE227 c(4x4): Sb rich interface

→ Low n-type doping leads to fewer heavy holes in Γ_8^{+v}

AE225:

- Amplitude at room temperature is 4x larger than at low temperatures.
- Below 150 K the amplitude remains constant.

AE227:

- Amplitude at room temperature is 2x as large as at low temperatures.
- Below 150 K the amplitude increases slightly.

The peak broadening decreases slightly with temperature for both samples.

Comparison with a Previous Study

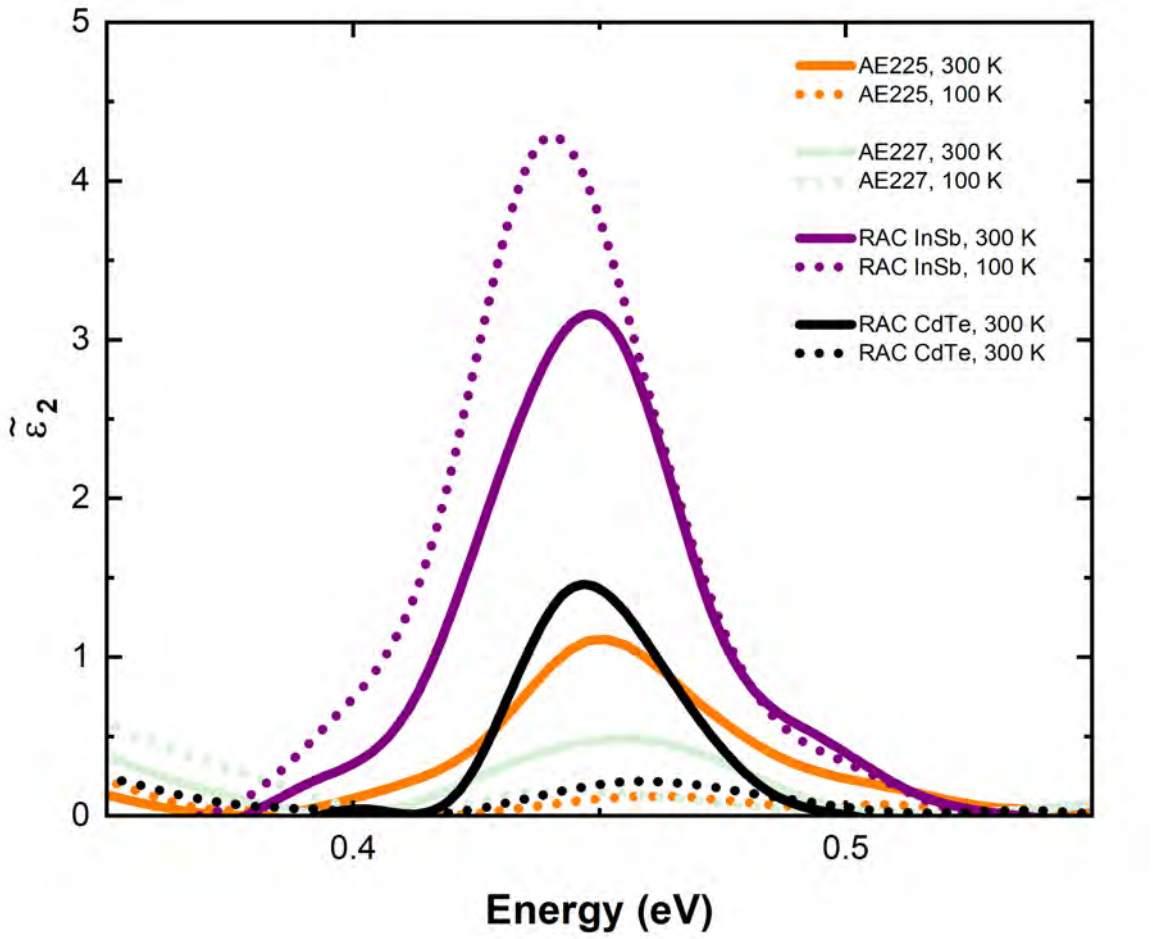

Name	Layers	Growth
AE225	**30 nm α-Sn / InSb (100) c(8x2)**	- **Atomic hydrogen clean at 285°C.** - **Anneal at 360°C.**
AE227	**30 nm α-Sn / InSb (100) c(4x4)**	- **Atomic hydrogen clean at 285°C.** - **Anneal at 430°C under Sb_4 flux.**
RAC InSb	70 nm α-Sn / InSb (100) c(8x2)	- Atomic hydrogen at 200°C.
RAC CdTe	70 nm α-Sn / CdTe (100) c(2x1)	- Slow anneal at 115 ° - RHEED monitors desorption of a-Te

- RAC InSb (heavily p-type doped) has the largest oscillator strength
- AE227 (n-type) has the smallest oscillator strength at high and low temperatures → the amplitude is below 0.5 for at 300 K and 100 K
- AE225 and RAC CdTe (intrinsic) have oscillator strengths with similar magnitudes at high and low temperatures.

→ We apply the f-sum rule using the integrated peak intensity and maximum contribution to find the hole density as a function of temperature.

[19]

Hole Density as a Function of Temperature

- The hole density was calculated using the same methods for all 4 samples.
- Theoretical values were calculated using the program explained in [38] for intrinsic α –Sn [38].

→ There is excellent agreement with the calculated values especially for the intrinsic samples.

→ RAC InSb shows significantly higher hole concentrations due to heavy p-type doping

→ AE227 has the lowest hole density that is only slightly reduced at low temperatures.

Sample	Type	p (10^{18} cm^{-3}) 300 K	p (10^{18} cm^{-3}) 100 K
SZ	intrinsic	3.67	0.61
AE225	intrinsic	3.56	0.38
AE227	n-type	1.50	0.75
RAC InSb	p-type	9.64	11.0
RAC CdTe	intrinsic	3.03	0.64

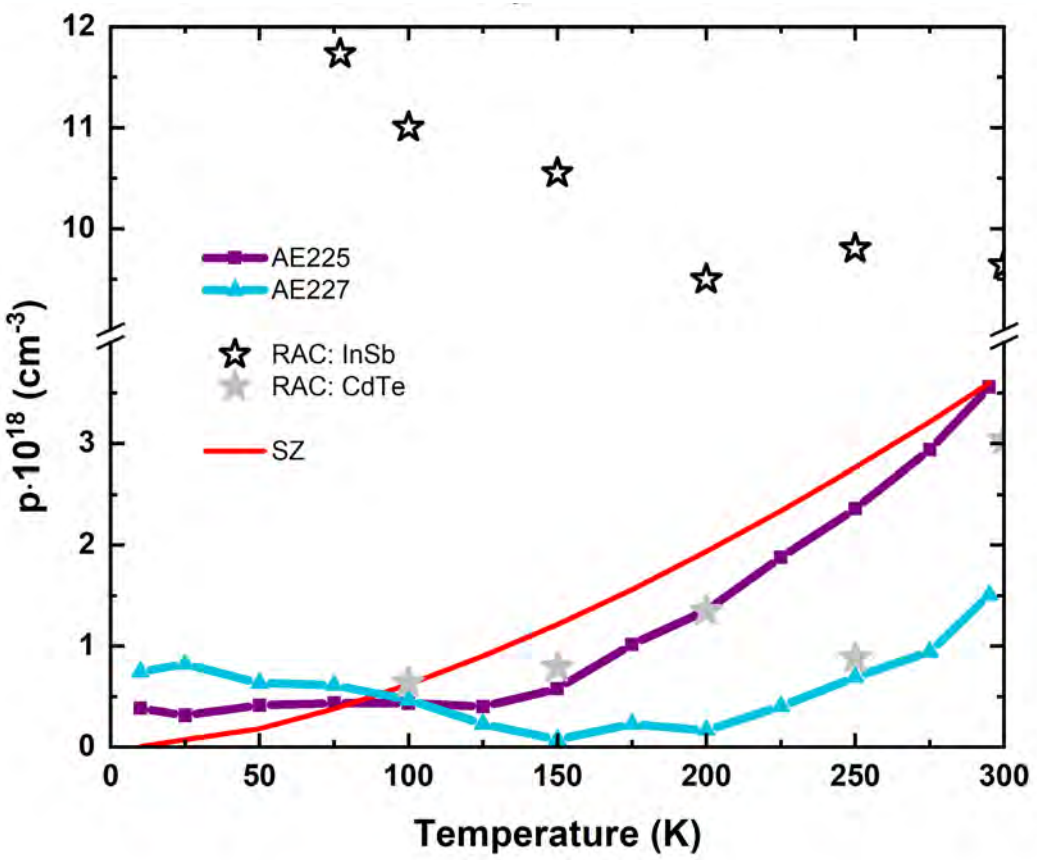

[38] S. Zollner. J. Vac. Sci. Technol. B 42 (2024), p. 022203.

Summary

- α-Sn has a tunable band structure and novel electronic properties … its very brittle and the critical temperature is low. → hard to work with
- It can be stabilized above the critical temperature by growing on a material with a lattice matched substrate such as InSb or CdTe

→ substrate material and interface preparation influence the band structure.

- Methods for determining carrier concentrations such as Hall effect measurements, or magneto reflectance measurements tend to be destructive and elaborate.

→ SE is a nondestructive method

- Modeling the dielectric function can be simplified with basis spline polynomials.
- The f-sum rule can be applied to the dielectric function to obtain the carrier density.

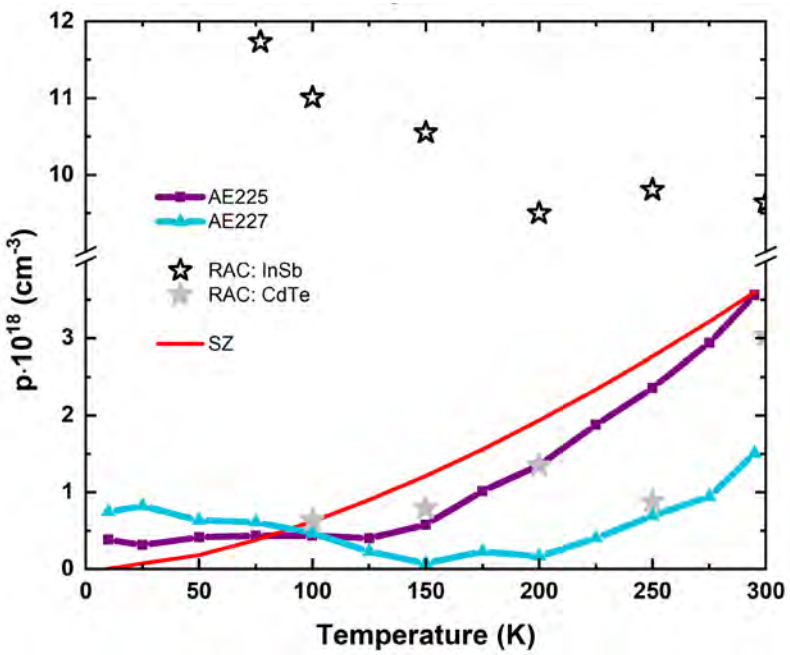

Sample	Type	p (10^{18} cm^{-3}) 300 K	p (10^{18} cm^{-3}) 100 K
SZ	intrinsic	3.67	0.61
AE225	intrinsic	3.558	0.376
AE227	n-type	1.504	0.746
RAC InSb	p-type	9.637	11.00
RAC CdTe	intrinsic	3.031	0.636